JBC RESEARCH ARTICLE

Expression of gamma-glutamyltransferase 1 in glioblastoma cells confers resistance to cystine deprivation–induced ferroptosis

Received for publication, December 9, 2021, and in revised form, February 2, 2022 Published, Papers in Press, February 8, 2022,
https://doi.org/10.1016/j.jbc.2022.101703

Kazuki Hayashima and Hironori Katoh*

From the Laboratory of Molecular Neurobiology, Graduate School of Biostudies, Kyoto University, Kyoto, Japan

Edited by Ruma Banerjee

Ferroptosis is an iron-dependent mode of cell death caused by excessive oxidative damage to lipids. Lipid peroxidation is normally suppressed by glutathione peroxidase 4, which requires reduced glutathione. Cystine is a major resource for glutathione synthesis, especially in cancer cells. Therefore, cystine deprivation or inhibition of cystine uptake promotes ferroptosis in cancer cells. However, the roles of other molecules involved in cysteine deprivation–induced ferroptosis are unexplored. We report here that the expression of gamma-glutamyltransferase 1 (GGT1), an enzyme that cleaves extracellular glutathione, determines the sensitivity of glioblastoma cells to cystine deprivation–induced ferroptosis at high cell density (HD). In glioblastoma cells expressing GGT1, pharmacological inhibition or deletion of GGT1 suppressed the cell density–induced increase in intracellular glutathione levels and cell viability under cystine deprivation, which were restored by the addition of cysteinylglycine, the GGT product of glutathione cleavage. On the other hand, cystine deprivation induced glutathione depletion and ferroptosis in GGT1-deficient glioblastoma cells even at an HD. Exogenous expression of GGT1 in GGT1-deficient glioblastoma cells inhibited cystine deprivation–induced glutathione depletion and ferroptosis at an HD. This suggests that GGT1 plays an important role in glioblastoma cell survival under cystine-limited and HD conditions. We conclude that combining GGT inhibitors with ferroptosis inducers may provide an effective therapeutic approach for treating glioblastoma.

Glioblastoma is the most common malignant brain tumor and has a poor prognosis (1, 2). Currently, surgical resection, radiation therapy, and chemotherapy are usually used to treat patients with glioblastoma. However, no effective treatment has been established, and the 5-year survival rate is only 5%. Therefore, it is important to find new effective therapeutic strategies for glioblastoma.

Ferroptosis is a form of cell death caused by excessive oxidative damage to lipids in an iron-dependent manner (3). It is well known that inhibition of glutathione peroxidase 4, an enzyme that directly reduces lipid peroxides, induces ferroptosis. The cystine/glutamate antiport system x_c^- is composed of two subunits, the light chain xCT (SLC7A11) with catalytic activity and the heavy chain CD98 (4F2hc or SLC3A2) with regulatory activity, and it exchanges extracellular cystine and intracellular glutamate at the plasma membrane (4, 5). In many cancer cells, cystine taken up by xCT is the major source of cysteine, which is required for the synthesis of reduced glutathione (GSH). As the activity of glutathione peroxidase 4 requires GSH, depletion of cystine or treatment with pharmacological inhibitors of xCT, such as erastin, induces ferroptosis (6). Therefore, the synthesis of GSH is important for the survival of cancer cells to avoid excessive oxidative stress and ferroptosis.

Gamma-glutamyltransferase (GGT) is a membrane-bound enzyme that is important for the metabolism of extracellular glutathione (7–9). GGT can cleave the gamma-glutamyl bond of glutathione to L-cysteinylglycine (Cys-Gly) and glutamate extracellularly, and Cys-Gly is further degraded into cysteine and glycine by dipeptidase and reused by being taken up into the cell. About 13 genes of the GGT family were identified using genomic and complementary DNA database searches (10). Among them, GGT1 is the most studied, and its expression increases in many human cancers, including glioblastoma (10, 11). Human GGT1 is autocatalytically cleaved into large and small subunits to generate the mature active enzyme (12, 13). Although inhibition of GGT1 was reported to inhibit the proliferation and migration of clear cell renal cell carcinoma cells (14), the role of GGT1 in cancer progression is still largely unknown. In this study, we demonstrated a role of GGT1 in ferroptosis resistance in glioblastoma cells cultured at a high density.

Results

High cell density suppresses cystine deprivation–induced ferroptosis in glioblastoma cells

We recently reported that cystine deprivation induces ferroptosis in glioblastoma cells (15). We found that this depends on cell density. Three types of glioblastoma cell lines, A172, T98G, and LN229, were plated at a low cell density (LD; 1×10^4 cells/cm^2) and high cell density (HD; 1×10^5 cells/cm^2) and cultured for 24 h. Then, the culture medium was collected at 24 h after cystine depletion, and the amount of lactate

* For correspondence: Hironori Katoh, hirokato@pharm.kyoto-u.ac.jp.

dehydrogenase (LDH) released into the medium was measured to quantify cell death. Depletion of cystine significantly increased cell death in all glioblastoma cell lines at LD. In LN229 cells, cystine deprivation also induced cell death at HD. However, it had little effect on cell viability in A172 and T98G cells at HD (Fig. 1*A*). The addition of ferroptosis inhibitors ferrostatin-1 (Fer-1) and deferoxamine (DFO) inhibited cell death under cystine deprivation in LN229 cells at HD (Fig. 1*B*). Our previous study revealed that cystine deprivation–induced ferroptosis involves two processes: depletion of intracellular GSH and degradation of ferritin in glioblastoma cells (15). Next, we examined whether the degradation of FTH1, the heavy chain subunit of ferritin, is affected by cell density. Western blotting of cell lysates after depletion of cystine confirmed that the protein levels of FTH1 decreased in both A172 and LN229 cells at LD and HD (Fig. 1*C*). On the other hand, we observed a difference in the levels of intracellular GSH between LD and HD. The intracellular GSH was depleted 15 h after cystine deprivation in three glioblastoma cell lines cultured at LD and in LN229 cells at HD. In contrast, the GSH levels decreased, but were not depleted, after cystine deprivation in A172 and T98G cells cultured at HD (Fig. 1*D*). L-buthionine sulfoximine (BSO), an inhibitor of γ-glutamylcysteine synthetase, the rate-limiting enzyme of GSH synthesis, depleted GSH and promoted cell death under cystine deprivation in A172 and T98G cells cultured at HD (Fig. 1, *E* and *F*). This suggests that cell density alters glutathione metabolism, which plays a role in the resistance to ferroptosis in A172 and T98G glioblastoma cells. On the other hand, BSO treatment depleted GSH but did not induce cell death in the presence of cystine. Our previous study suggests that BSO did not induce ferritinophagy required for the induction of ferroptosis in the presence of cystine in glioblastoma cells (15). Therefore, BSO promoted cell death in A172 and T98G cells at HD only in the absence of cystine.

We next examined whether the medium from HD culture can inhibit cystine deprivation–induced cell death at LD. The medium from A172 or T98G culture at HD (HD conditioned medium) suppressed cystine deprivation–induced cell death in A172 or T98G cells cultured at LD, whereas HD conditioned medium from LN229 culture had little effect on cystine deprivation–induced cell death in LN229 cells cultured at LD (Fig. 1*G*). Therefore, factors secreted from A172 or T98G cells at HD can alter cell viability under cystine deprivation.

Inhibition of GGT1 promotes cystine deprivation–induced ferroptosis at HD

Glutathione is synthesized in the cytoplasm, but it is also exported out of the cell (16). We next examined whether GGT, an enzyme that degrades glutathione to Cys-Gly and glutamate extracellularly, is involved in the cystine deprivation–induced cell death at HD. OU749, an inhibitor of GGT, significantly increased the percentage of cell death under cystine deprivation in A172 and T98G cells at HD (Fig. 2*A*). In LN229 cells, cystine deprivation induced cell death at HD in the presence or the absence of OU749. The ferroptosis inhibitors Fer-1 and DFO inhibited OU749-induced cell death under cystine deprivation in A172 cells at HD (Fig. 2*B*), suggesting that OU749 induces ferroptotic cell death under cystine deprivation at HD. In addition, OU749 depleted GSH in cystine-deprived A172 and T98G cells cultured at HD (Fig. 2*C*). In LN229 cells, cystine deprivation induced GSH depletion at HD in the presence or the absence of OU749. We therefore hypothesized that the function of GGT caused a significant difference between A172/T98G cells and LN229 cells in ferroptosis sensitivity. Human GGT1, the most widely expressed member of the GGT family, is autocatalytically cleaved into large and small subunits to generate the mature active enzyme (12, 13). We compared the expression levels of GGT1 by Western blotting with an antibody against the small subunit and found that GGT1 was expressed in A172 and T98G cells. However, expression of GGT1 was undetectable in LN229 cells (Fig. 2*D*). The protein levels of GGT1 in A172 and T98G cells were unaffected when they were cultured at HD (Fig. 2*E*). We next generated GGT1-deficient A172 cells using CRISPR/Cas9-mediated deletion of GGT1 (A172 GGT1 KO 1 and 2; Fig. 2*F*). In A172 control KO cells, cystine deprivation did not induce cell death when cultured at HD. However, cystine deprivation significantly increased cell death in A172 GGT1 KO 1 and 2 cells at HD (Fig. 2*G*). In addition, cystine deprivation reduced the GSH level to less than 10% in GGT1 KO 1 and 2 cells at HD, whereas it reduced the GSH level to approximately 40% in control KO cells, which were depleted by OU749 (Fig. 2*H*). This suggests that GGT1 plays an important role in GSH metabolism and resistance to ferroptosis in glioblastoma cells at HD.

Extracellular Cys-Gly suppresses cystine deprivation–induced cell death at HD

GGT1 cleaves extracellular glutathione to produce Cys-Gly and glutamate (16, 17). Therefore, we next examined whether Cys-Gly restored cell viability in A172 cells treated with OU749. The addition of Cys-Gly to the medium suppressed OU749-induced cell death in A172 cells under cystine deprivation at HD. Cys-Gly also suppressed cystine deprivation–induced cell death in LN229 cells at HD in the absence or the presence of OU749 (Fig. 3*A*). High concentration of glutamate inhibits xCT-mediated cystine uptake (4, 18, 19). However, addition of glutamate at the same concentration of Cys-Gly (100 μM) had little effect on the cell viability (Fig. 3*B*). We confirmed the effect of extracellular glutamate on cystine uptake in A172 cells. The xCT inhibitor sulfasalazine (SSZ) completely suppressed cystine uptake in A172 cells, but glutamate treatment at 100 μM did not (Fig. 3*C*), suggesting that a higher concentration of extracellular glutamate is required for inhibition of cystine import through xCT. On the other hand, the addition of GSH had little effect on OU749-induced cell death in A172 cells under cystine deprivation at HD or on cystine deprivation–induced cell death in LN229 cells at HD in the absence or the presence of OU749 (Fig. 3*D*). We used A172 GGT1 KO 1 cells to confirm the effect of Cys-Gly on cell viability. In A172 GGT1 KO 1 cells

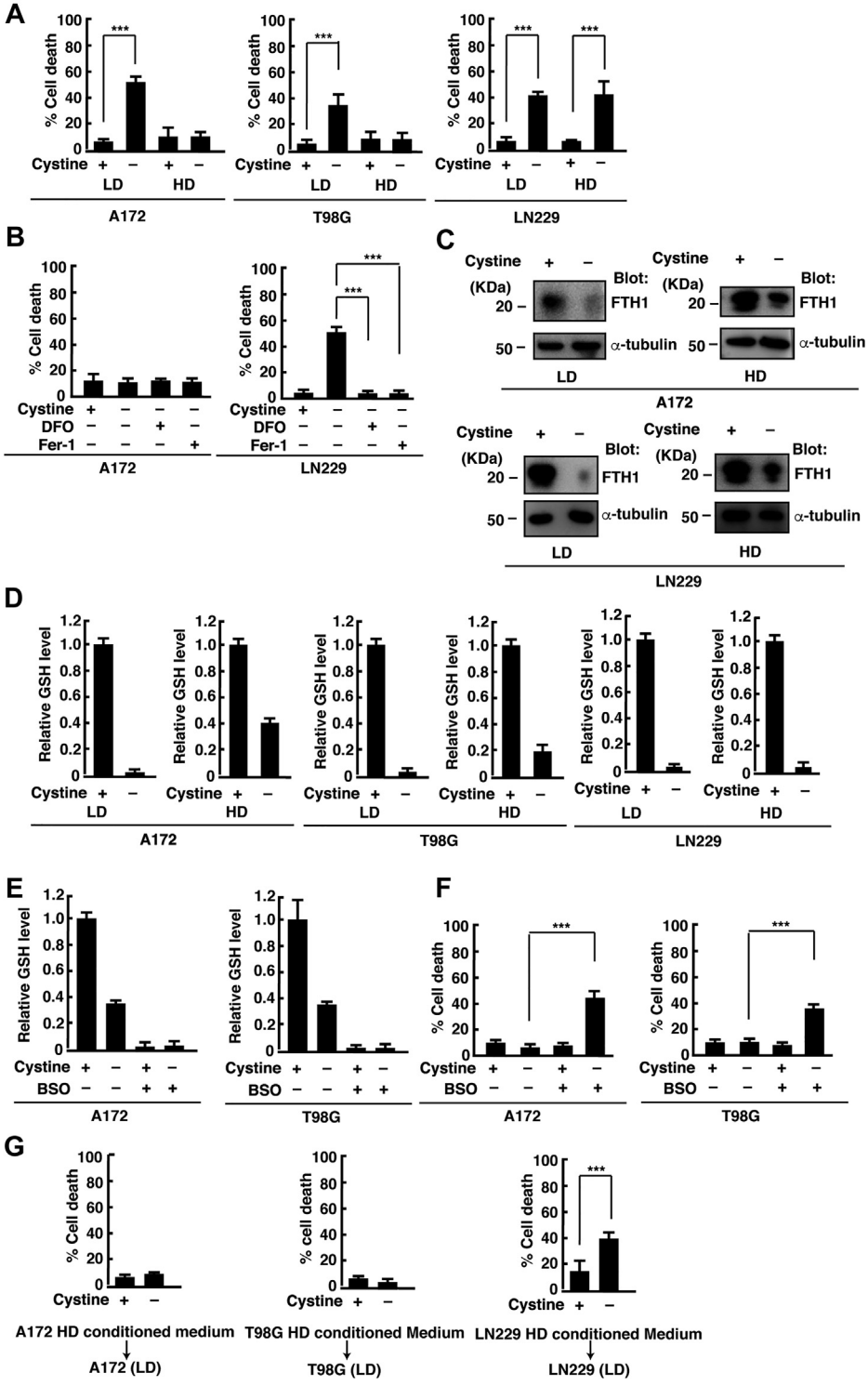

Figure 1. HD suppresses cystine deprivation–induced ferroptosis in glioblastoma cells. *A*, A172, T98G, and LN229 cells were cultured at LD (1×10^4 cells/cm^2) or HD (1×10^5 cells/cm^2) for 24 h and placed in cystine-free medium with or without cystine (200 μM) for 24 h. *B*, A172 and T98G cells were cultured at HD for 24 h and treated with DFO (100 μM) or Fer-1 (1 μM) in cystine-free medium for 24 h. Cell death was quantified using an LDH release assay. Cells treated with 0.1% Tween-20 were used to calculate 100% cell death. Error bars represent SD (n = 3). ***$p < 0.001$; calculated by one-way ANOVA with Tukey's post hoc test. *C*, immunoblot analysis of A172 and LN229 cells cultured at LD or HD for 24 h and placed in cystine-free medium with or without cystine (200 μM) for 15 h. *D*, A172, T98G, and LN229 cells were cultured at LD or HD for 24 h and placed in cystine-free medium with or without cystine (200 μM) for 15 h. *E*, A172 and T98G cells were cultured at HD for 24 h and placed in cystine-free medium with or without cystine (200 μM) or treated with or without BSO (100 μM) for 15 h. Intracellular GSH levels relative to control (+cystine) are shown. Error bars represent SD (n = 3). *F*, A172 and T98G cells were cultured at HD for 24 h and placed in cystine-free medium with or without cystine (200 μM) or treated with or without BSO (100 μM) for 24 h. *G*, A172, T98G, and LN229 cells cultured at LD were placed in the conditioned medium collected from the cells cultured at HD in cystine-free medium with or without cystine (200 μM) for 24 h. Cell death was quantified using an LDH release assay. Cells treated with 0.1% Tween-20 were used to calculate 100% cell death. Error bars represent SD (n = 3). ***$p < 0.001$; calculated by one-way ANOVA with Tukey's post hoc test. BSO, L-buthionine sulfoximine; DFO, oxamine; Fer-1, ferrostatin-1; GSH, reduced glutathione; HD, high cell density; LD, low cell density; LDH, lactate dehydrogenase.

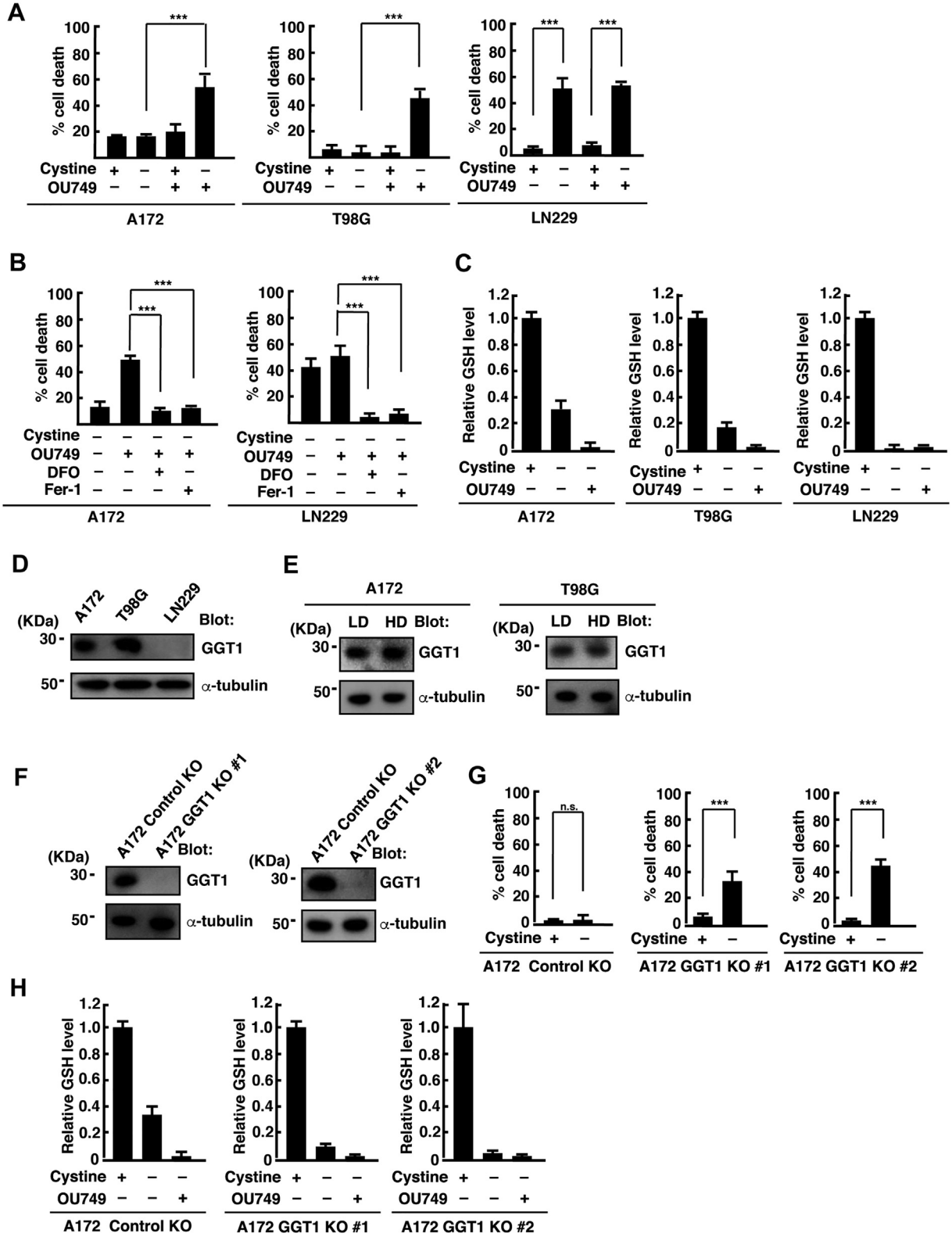

Figure 2. Inhibition of GGT1 promotes cystine deprivation–induced ferroptosis at HD. *A*, A172, T98G, and LN229 cells were cultured at HD for 24 h and placed in cystine-free medium with or without cystine (200 μM) and OU749 (250 μM) for 24 h. *B*, A172 and LN229 cells were cultured at HD for 24 h and placed in cystine-free medium with or without OU749 (250 μM), DFO (100 μM), and Fer-1 (1 μM) for 24 h. Quantification of cell death was performed using an LDH release assay. Cells treated with 0.1% Tween-20 were used to calculate 100% cell death. Error bars represent SD (n = 3). ***$p < 0.001$; calculated by one-way ANOVA with Tukey's post hoc test. *C*, A172, T98G, and LN229 cells were cultured at HD for 24 h and placed in cystine-free medium with or without cystine (200 μM) and OU749 (250 μM) for 15 h. Intracellular GSH levels relative to control (+cystine) are shown. Error bars represent SD (n = 3). *D*, immunoblot analysis of A172, T98G, and LN229 cell lysates. *E*, immunoblot analysis of A172 and T98G cell lysates cultured at LD or HD for 24 h. *F*, immunoblot analysis of A172 control KO, GGT1 KO 1, and GGT1 KO 2 cell lysates. *G*, A172 control KO and GGT1 KO (1 and 2) cells were cultured at HD for 24 h and placed in cystine-free medium with or without cystine (200 μM) for 24 h. Cell death was quantified using an LDH release assay. Error bars represent

cultured at HD, cystine deprivation induced cell death in the presence and absence of OU749, which was greatly inhibited by Cys-Gly (Fig. 3*E*). Like parental cells, OU749 increased cell death in cystine-deprived A172 control cells at HD, which was suppressed by Cys-Gly. The addition of GSH did not affect cell viability in cystine-deprived A172 GGT1 KO 1 and control KO cells at HD (Fig. 3*F*). We next examined the effects of extracellular Cys-Gly on the intracellular GSH levels in A172 and LN229 cells. Cystine deprivation together with OU749 depleted intracellular GSH in A172 cells at HD. The addition of Cys-Gly significantly increased the intracellular GSH level, whereas the addition of GSH did not (Fig. 3*G*). Similarly, Cys-Gly but not GSH increased the intracellular GSH level in cystine-deprived LN229 cells and A172 GGT1 KO 1 cells at HD (Fig. 3, *G* and *H*). In A172 control KO cells, the addition of GSH also increased the intracellular GSH level in the absence of OU749. This suggests that GGT1-mediated formation of Cys-Gly suppresses cystine deprivation–induced cell death in glioblastoma cells at HD.

Serine is a major donor of one-carbon metabolism and used for an alternative pathway of glutathione synthesis (20). To examine whether *de novo* serine synthesis is involved in the maintenance of GSH levels under cystine deprivation at HD, we used NCT-503, a specific inhibitor of phosphoglycerate dehydrogenase. Phosphoglycerate dehydrogenase is the enzyme that catalyzes the first step of serine synthesis from the glycolytic intermediate 3-phosphoglycerate. Treatment with NCT-503 slightly decreased the GSH levels in A172 and T98G cells at HD in the presence and absence of cystine, and they were depleted by adding OU749 (Fig. 3*I*). This suggests that *de novo* serine synthesis from the glycolytic intermediate plays a role in an alternative pathway for GSH synthesis in glioblastoma cells.

GGT1 regulates the degradation of extracellular glutathione at HD

To examine whether GGT1 regulates extracellular glutathione levels in glioblastoma cells, we next measured the amounts of the oxidized glutathione (GSSG) and GSH forms of glutathione in the medium. The levels of GSH in the medium were low in A172 and LN229 cells at both LD and HD with or without cystine (Fig. 4*A*). Thus, most glutathione in the medium was present in the oxidized form, and it was not affected by cystine deprivation or OU749 treatment (Fig. 4*B*). The extracellular concentrations of GSSG were high at HD, and they were reduced by cystine deprivation (Fig. 4*A*). OU749 restored the extracellular glutathione to the level in the presence of cystine in A172 cells at HD, but it had no effect on the extracellular glutathione levels in A172 cells at LD or in LN229 cells at LD and HD (Fig. 4*C*). The level of extracellular glutathione was also high in cystine-deprived A172 GGT1 KO 1 cells (Fig. 4*D*). This suggests that GGT1 promotes the degradation of extracellular glutathione in cystine-deprived glioblastoma cells cultured at HD. The intracellular cysteine levels were not significantly different between LD and HD in A172 and LN229 cells (Fig. 4*E*). In addition, the level of secreted glutathione per cell is similar between LD and HD in A172 cells (LD, 2.71×10^{-14} mol per cell; HD, 2.14×10^{-14} mol per cell).

As described previously, the medium from A172 HD cultures inhibited cystine deprivation–induced cell death at LD. When A172 cells were cultured at HD in the presence of OU749, the medium did not inhibit cystine deprivation–induced cell death at LD. However, the addition of Cys-Gly to the medium from OU749-treated HD cultures restored cell viability of A172 cells at LD (Fig. 4*F*). In addition, the effects of Cys-Gly on cell viability were concentration dependent in both A172 and LN229 cells at HD (Fig. 4*G*). Thus, glutathione and its metabolite Cys-Gly are factors in the medium from A172 cells at HD that alter cell viability under cystine deprivation.

Exogenous expression of GGT1 increases cell viability under cystine deprivation at HD

The expression of GGT1 was undetectable in LN229 cells. Therefore, we generated LN229 cells that stably expressed GGT1 (LN229 GGT1; Fig. 5*A*) and examined whether they acquire resistance to ferroptosis at HD. In control LN229 cells expressing the empty vector (LN229 control), cystine deprivation induced cell death at LD and HD. On the other hand, cystine deprivation did not induce cell death in LN229 GGT1 cells at HD, although it induced cell death at LD (Fig. 5*B*). Treatment with the GGT inhibitor OU749 restored cell death in LN229 GGT1 cells at HD (Fig. 5*C*). Intracellular GSH was depleted under cystine deprivation in LN229 control cells cultured at HD, whereas the GSH level decreased, but was not depleted, after cystine deprivation in LN229 GGT1 cells cultured at HD (Fig. 5*D*). OU749 depleted GSH in cystine-deprived LN229 GGT1 cells cultured at HD (Fig. 5*E*), suggesting that exogenous expression of GGT1 increases glioblastoma cell viability under cystine deprivation at HD.

Discussion

The survival of cancer cells depends on their ability to adapt to environmental conditions. In this study, we found that GGT1, an enzyme responsible for the extracellular degradation of glutathione, plays a major role in the survival of glioblastoma cells under cystine-deficient conditions. Glioblastoma cells with high expression of GGT1 can survive under cystine deprivation conditions when they are cultured at HD. This is due in part to higher intracellular GSH levels even without cystine in the medium. Indeed, inhibition of GGT1 activity by the GGT inhibitor OU749 or CRISPR-mediated deletion or inhibition of GSH synthesis induced the

SD (n = 3). ***$p < 0.001$; ns; calculated by one-way ANOVA with Tukey's post hoc test. *H*, A172 control KO and GGT1 KO (1 and 2) cells were cultured at HD for 24 h and placed in cystine-free medium with or without cystine (200 μM) and OU749 (250 μM) for 15 h. Intracellular GSH levels relative to control (+cystine) are shown. Error bars represent SD (n = 3). DFO, deferoxamine; Fer-1, ferrostatin-1; GGT1, gamma-glutamyltransferase 1; GSH, reduced glutathione; HD, high cell density; LDH, lactate dehydrogenase; ns, not significant.

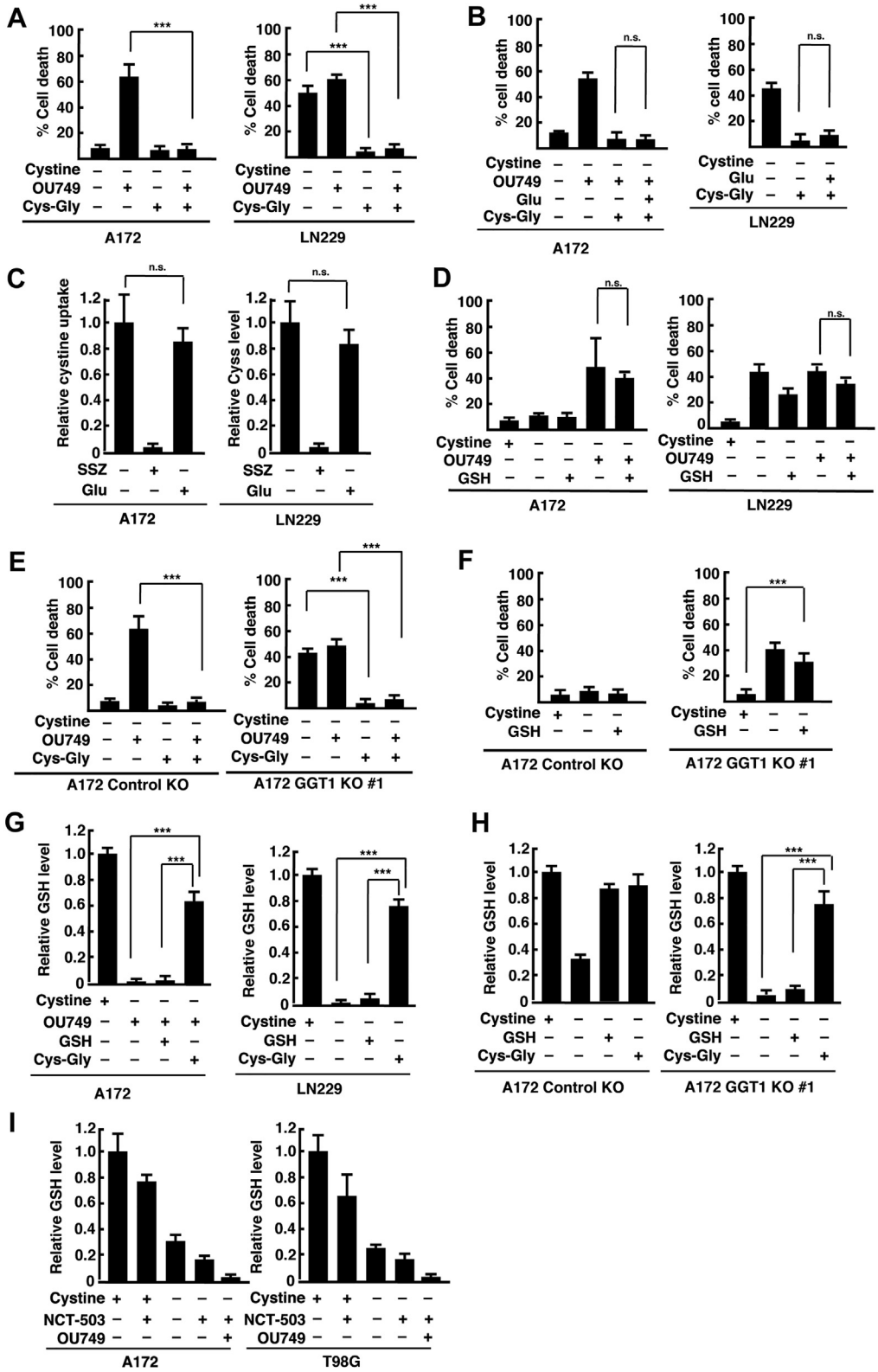

Figure 3. Extracellular cysteinylglycine (Cys-Gly) suppresses cystine deprivation–induced cell death at HD. *A* and *B*, A172 and LN229 cells were cultured at HD for 24 h and placed in cystine-free medium with or without cystine (200 μM), OU749 (250 μM), Cys-Gly (100 μM), and glutamate (Glu, 100 μM) for 24 h. Cell death was quantified using an LDH release assay. Error bars represent SD (n = 3). ***$p < 0.001$; ns; calculated by one-way ANOVA with Tukey's post hoc test. *C*, fluorescence assay of cystine uptake in A172 and LN229 cells treated with SSZ (250 μM) or glutamate (Glu, 100 μM). Error bars represent SD (n = 3). ns; calculated by one-way ANOVA with Tukey's post hoc test. *D*, A172 and LN229 cells were cultured at HD for 24 h and placed in cystine-free medium with or without cystine (200 μM), OU749 (250 μM), Cys-Gly (100 μM), and GSH (100 μM) for 24 h. *E* and *F*, A172 control KO and GGT1 KO 1 cells were cultured at HD for 24 h and placed in cystine-free medium with or without cystine (200 μM), OU749 (250 μM), Cys-Gly (100 μM), and GSH (100 μM) for 24 h. Cell death was quantified using an LDH release assay. Error bars represent SD (n = 3). ***$p < 0.001$; ns; calculated by one-way ANOVA with Tukey's post hoc test. *G*, A172 and LN229 cells were cultured at HD for 24 h and placed in cystine-free medium with or without cystine (200 μM), OU749

depletion of intracellular GSH and increased cell death in cystine-deprived glioblastoma cells at HD. The medium from HD cultures of glioblastoma cells contained a high concentration of glutathione, which is converted to Cys-Gly and glutamate by GGT1. The addition of Cys-Gly to the medium restored GSH levels and cell viability in the presence of OU749 or in GGT1-deficient cells. Furthermore, ectopic expression of GGT1 in GGT1-deficient cells increased cell viability under cystine deprivation conditions at HD. Taken together, our study suggests that the higher expression of GGT1 is responsible for resistance to cystine deprivation–induced ferroptosis in glioblastoma cells at HD. Glutathione is exported to the extracellular space and converted to Cys-Gly through GGT, and Cys-Gly is then converted to cysteine through dipeptidase. Extracellular cysteine is reoxidized to cystine, which is taken up into cells *via* xCT and reused for synthesis of GSH (21). Thus, glutathione cycling, which depends on GGT, helps glioblastoma cells to maintain intracellular GSH pool for ferroptosis protection during cystine starvation conditions (Fig. 5*F*). Therefore, cystine depletion together with the inhibition of GGT activity may be an attractive therapeutic strategy for glioblastoma. On the other hand, Cys-Gly inhibits cystine deprivation–induced cell death in a concentration-dependent manner, suggesting that higher concentrations of glutathione and its metabolite Cys-Gly in the extracellular space are required for suppression of ferroptosis under cystine deprivation conditions. The more cells seeded in the dish, the more glutathione secreted from cells into medium, resulting in higher extracellular glutathione concentrations in medium. Therefore, we need to study this in the context of HD.

Cancer cells contain high levels of GSH, which supports cell proliferation, metastasis, and stress resistance. In addition to its role as an antioxidant, GSH is involved in the maintenance of cysteine pools because an excess amount of intracellular cysteine is toxic to cells (22–24). GGT functions in the recycling of cysteine from GSH, and several studies reported that cancer cells overexpressing GGT utilize extracellular GSH as a source of intracellular cysteine and GSH (17, 25–27). Indeed, deletion of GGT1 expression in glioblastoma cells led to the depletion of intracellular GSH under cystine deprivation, suggesting that glioblastoma cells utilize extracellular glutathione for the maintenance of intracellular GSH when they are unable to obtain extracellular cystine. It was also reported that GGT1 is highly expressed in numerous cancers, including glioblastoma (10, 11). In particular, GGT1 is detected in exosomes from cancer cells, and serum exosomal GGT activity was reported to be a useful biomarker for several types of cancer (28, 29). Therefore, it is important for future studies to investigate whether GGT1 in exosomes from HD glioblastoma cells plays a role in the resistance to ferroptosis.

It is well known that cellular conditions affect cell viability. In particular, contact inhibition and HD culture affect cell survival and proliferation. One of the key mechanisms controlling contact inhibition is the Hippo signaling pathway. When cells are seeded at HD, the Hippo signaling pathway is activated, causing the transfer of Yes-associated protein (YAP)/transcriptional coactivator with PDZ-binding motif (TAZ) from the nucleus to the cytosol and their inactivation, and cell proliferation is stopped (30–32). Cancer cells lose contact inhibition and induce dysregulated proliferation. However, cell density has also been reported to affect cancer cell viability. For example, HD causes drug resistance and increases cell viability of many cancer cells, including glioblastoma (33–35). HD culture also protects cancer cells from glucose deprivation–induced cell death (36). On the other hand, recent studies reported that the activation of YAP and TAZ increases the expression of genes involved in ferroptosis, such as ACSL4, and increases cancer cell susceptibility to ferroptosis. HD-induced activation of the Hippo pathway inactivates YAP/TAZ, leading to resistance to ferroptosis (37–39). The expression of GGT1 in glioblastoma cells was unaffected when cultured at HD, suggesting that GGT1-mediated resistance to ferroptosis at HD is independent of the Hippo pathway. Further studies are needed to clarify the relationship between glutathione metabolism and the Hippo pathway in ferroptosis resistance in cancer cells.

Experimental procedures

Plasmids and reagents

The expression plasmid pCXN2 vector was a generous gift from Dr J. Miyazaki (Osaka University). The coding sequence of human GGT1 was amplified from HeLa cells by reverse transcription–PCR and subcloned into pCXN2. The single-guide RNAs (sgRNAs) targeting human GGT1 sequence (#1, 5′-actgcgggacggtggctctg-3′; #2, 5′-ctgcttggcatccgcggcca-3′) were cloned into the sgRNA expression vector peSpCAS9(1.1)-2xsgRNA (Addgene; plasmid no.: 80768). Cystine-free medium was prepared as described previously (15). Inhibitors and amino acid compounds were used at the following concentrations: BSO, 100 μM; DFO, 100 μM (Santa Cruz Biotechnology); Fer-1, 1 μM; SSZ, 250 μM; Cys-Gly, 100 μM; glutamate, 100 μM (Sigma–Aldrich); OU749, 250 μM; NCT-503, 25 μM (Cayman); and GSH (Nacalai Tesque, Inc), 100 μM.

Cell culture and transfection

A172 and T98G cell lines were provided by the RIKEN BioResource Research Center through the National BioResource Project of the Ministry of Education, Culture, Sports, Science and Technology of Japan (T98G, RCB1954;

(250 μM), Cys-Gly (100 μM), and GSH (100 μM) for 15 h. *H*, A172 control KO and GGT1 KO cells were cultured at HD for 24 h and placed in cystine-free medium with or without cystine (200 μM), Cys-Gly (100 μM), and GSH (100 μM) for 15 h. *I*, A172 and T98G cells were cultured at HD for 24 h and placed in cystine-free medium with or without cystine (200 μM), NCT-503 (25 μM), and OU749 (250 μM) for 15 h. Intracellular GSH levels relative to control (+cystine) are shown. Error bars represent SD (n = 3). ***$p < 0.001$; calculated by one-way ANOVA with Tukey's post hoc test. GGT1, gamma-glutamyltransferase 1; GSH, reduced glutathione; HD, hugh cell density; LDH, lactate dehydrogenase; ns, not significant; SSZ, sulfasalazine.

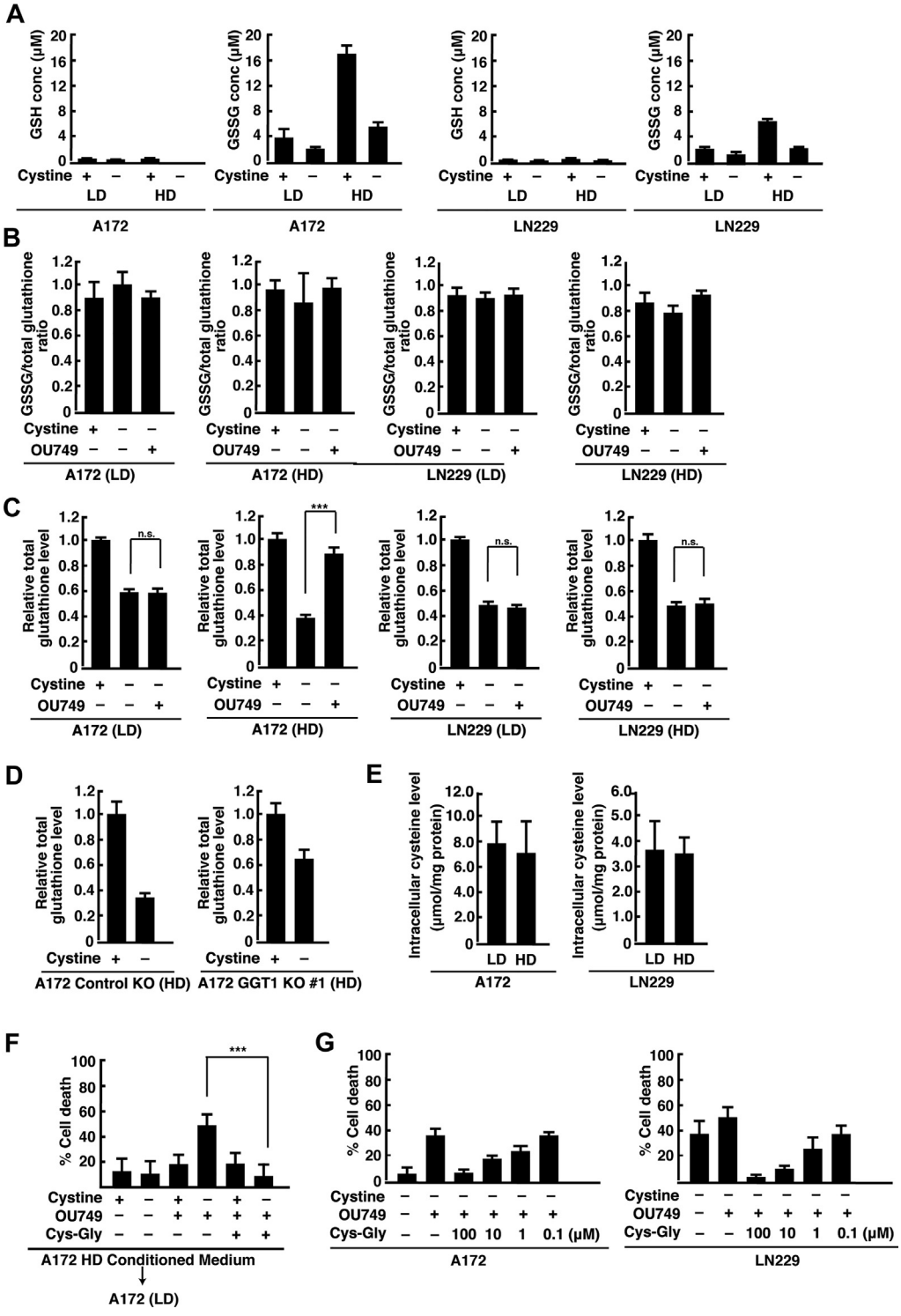

Figure 4. GGT1 regulates the degradation of extracellular glutathione at HD. *A*, A172 and LN229 cells were cultured at LD or HD for 24 h and placed in cystine-free medium with or without cystine (200 μM) for 15 h. The concentrations of GSH and GSSG in the medium were measured. *B*, A172 and LN229 cells were cultured at LD or HD for 24 h and placed in cystine-free medium with or without cystine (200 μM) and OU749 (250 μM) for 15 h. The ratio of GSSG to total glutathione in the medium was measured. *C*, A172 and LN229 cells were cultured at LD or HD for 24 h and placed in cystine-free medium with or without cystine (200 μM) and OU749 (250 μM) for 15 h. Total glutathione levels relative to control (+cystine) in the medium are shown. *D*, A172 control KO and GGT1 KO 1 cells were cultured at HD for 24 h and placed in cystine-free medium with or without cystine (200 μM) for 15 h. Total glutathione levels relative to control (+cystine) in the medium are shown. *E*, cytosolic cysteine levels in A172 and LN229 cells at LD and HD. *F*, A172 cells cultured at LD were placed in the conditioned medium collected from the cells cultured at HD in cystine-free medium with or without cystine (200 μM), OU749 (250 μM), and Cys-Gly (100 μM) for 24 h. *G*, A172 and LN229 cells were cultured at HD for 24 h and placed in cystine-free medium with or without OU749 (250 μM) and the indicated concentrations of Cys-Gly for 24 h. Cell death was quantified using an LDH release assay. Cells treated with 0.1% Tween-20 were used to calculate 100% cell death. Error bars represent SD (n = 3). ***$p < 0.001$; ns; calculated by one-way ANOVA with Tukey's post hoc test. Cys-Gly, l-cysteinylglycine; GGT1, gamma-glutamyltransferase 1; GSH, reduced glutathione; GSSG, oxidizedione; HD, high cell density; LD, low cell density; LDH, lactate dehydrogenase; ns, not significant.

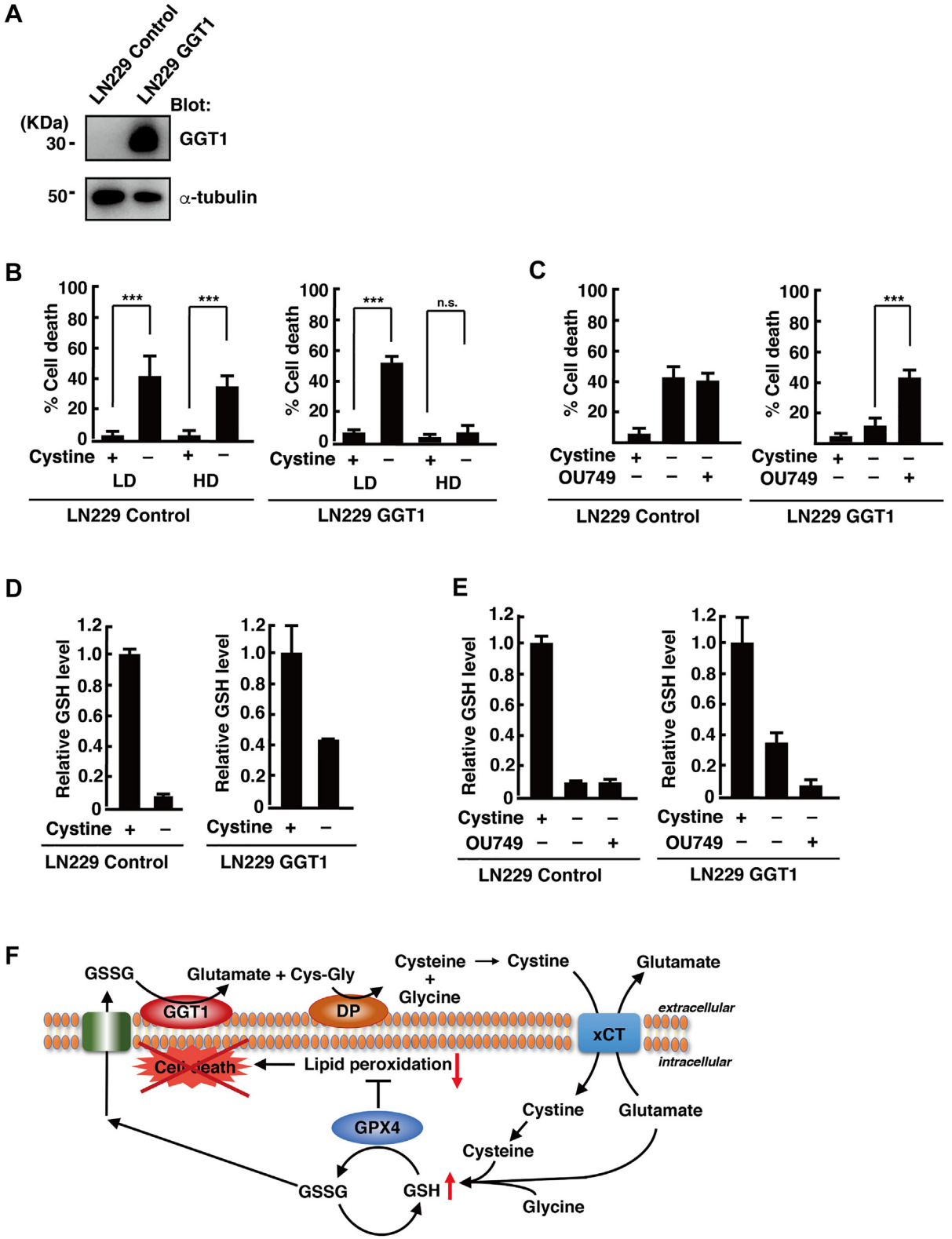

Figure 5. Exogenous expression of GGT1 increases cell viability under cystine deprivation at HD. *A*, immunoblot analysis of LN229 control and GGT1 cell lysates. *B* and *C*, LN229 control and GGT1 cells were cultured at LD or HD for 24 h and placed in cystine-free medium with or without cystine (200 μM) and OU749 (250 μM) for 24 h. Cell death was quantified using an LDH release assay. Cells treated with 0.1% Tween-20 were used to calculate 100% cell death. *D* and *E*, LN229 control and GGT1 cells were cultured at LD or HD for 24 h and placed in cystine-free medium with or without cystine (200 μM) and OU749 (250 μM) for 15 h. Intracellular GSH levels relative to control (+cystine) are shown. Error bars represent SD (n = 3). ***$p < 0.001$; ns; calculated by one-way ANOVA with Tukey's post hoc test. *F*, model of GGT1-mediated resistance to ferroptosis under cystine deprivation conditions. GGT1, gamma-glutamyltransferase 1; GSH, reduced glutathione; HD, high cell density; LD, low cell density; LDH, lactate dehydrogenase; ns, not significant.

A172, RCB2530). LN229 cell line was obtained from American Type Culture Collection (no.: CRL-2611). Cells were cultured in Dulbecco's modified Eagle's medium containing 10% fetal bovine serum, 4 mM glutamine, 100 units/ml penicillin, and 0.1 mg/ml streptomycin under humidified air with 5% CO_2 at 37 °C. Transfection was performed using Lipofectamine 2000 (Life Technologies). To generate A172 GGT1 KO cells, we used the CRISPR/Cas9-mediated homology-independent knock-in system (40). A172 cells seeded in dishes of 60 mm (250,000 cells/dish) were transfected with peSpCAS9(1.1)-2xsgRNA containing sgRNA targeting human GGT1 and pDonor-tBFP-NLS-Neo (Addgene; plasmid no.: 80766). To generate LN229 GGT1 cells, cells seeded in dishes of 60 mm (250,000 cells/dish) were transfected with pCXN2-GGT1. Two days after transfection, cells were collected and seeded onto dishes of 100 mm with medium containing 300 μg/ml of G418 (Wako) to remove untransfected cells. About 10 days after selection, colonies grown from single cells were isolated. These clones were expanded and screened by immunoblotting using anti-GGT1 antibody.

Cell death experiments

Cystine deprivation was performed as described previously (15). Cell death was measured using the MTX LDH kit (Kyokuto Pharmaceutical Industries) according to the manufacturer's instructions. The absorbance was measured at 595 nm using a microplate reader (Tecan Genesis). Cells treated with 0.1% Tween 20 represented 100% cell death.

Measurement of glutathione

The amount of intracellular GSH was measured using the GSH-Glo Glutathione Assay (Promega) according to the manufacturer's instructions. The luminescence was measured using a microplate reader (Tecan Genesis). A black 96-well plate was used to prevent light from leaking into the adjacent wells. The amounts of extracellular total and GSSG were measured using the GSH–GSSG Glutathione Assay (Promega).

Measurement of intracellular cysteine

Cells cultured in 48-well plates at LD or HD were collected with PBS. After centrifugation, the cells were suspended in H_2O and disrupted by ultrasonication on ice with TOMY Handy Sonic (model UR-20P) at the amplitude of 20% for 1 min. The cytosolic cysteine was measured using the cysteine assay kit (MAK255; Sigma–Aldrich) according to the manufacturer's instructions. The fluorescence was measured using the Tecan microplate reader. A black 96-well plate was used to prevent light from leaking into the adjacent wells. Protein concentration was measured using the Protein Assay BCA Kit (Nacalai Tesque, Inc).

Measurement of cystine uptake

Cystine uptake was measured using the Cystine uptake assay kit (Dojindo Laboratories) according to the manufacturer's instructions (41). The fluorescence was measured using the Tecan microplate reader. A black 96-well plate was used to prevent light from leaking into the adjacent wells.

Immunoblotting and antibodies

Cells were lysed with Laemmli sample buffer and analyzed by immunoblotting as described previously (15). Signals were captured by Amersham Imager 600 (GE Healthcare Life Sciences). The following antibodies were used in this study: GGT1/2 (sc-393706; Santa Cruz Biotechnology); FTH1 (4393; Cell Signaling Technology); anti-α-tubulin antibody (T5168; Sigma–Aldrich); secondary antibodies conjugated to horseradish peroxidase against mouse immunoglobulin G (P0447; DAKO) and rabbit immunoglobulin G (P0448; DAKO).

Data analysis

Data were analyzed using ANOVA and Tukey's honest significant difference post hoc test. $p < 0.05$ was considered significant. Statistical analysis was performed using KaleidaGraph (Synergy Software).

Data availability

All data are contained within the article.

Acknowledgments—We thank Prof Junichi Miyazaki (Osaka University, Osaka, Japan) for the CAG promoter–containing vector. We also thank Dr Yohei Katoh and Prof Kazuhisa Nakayama (Kyoto University) for providing peSpCAS9(1.1)-2xsgRNA and pDonor-tBFP-NLS-Neo. This study was supported in part by Grants-in-aid for Scientific Research from the Japan Society for the Promotion of Science (grant nos.: 18K06215 and 21K06065).

Author contributions—K. H. and H. K. conceptualization; K. H. and H. K. methodology; K. H. and H. K. formal analysis; K. H. and H. K. investigation; K. H. and H. K. resources; K. H. and H. K. data curation; K. H. and H. K. writing–original draft; K. H. and H. K. writing–review & editing; K. H. and H. K. visualization; H. K. project administration; H. K. funding acquisition.

Conflict of interest—The authors declare that they have no conflicts of interest with the contents of this article.

Abbreviations—The abbreviations used are: BSO, L-buthionine sulfoximine; Cys-Gly, L-cysteinylglycine; DFO, deferoxamine; Fer-1, ferrostatin-1; GGT1, gamma-glutamyltransferase 1; GSH, reduced glutathione; GSSG, oxidized glutathione; HD, high cell density; LD, low cell density; LDH, lactate dehydrogenase; sgRNA, single-guide RNA; SSZ, sulfasalazine; TAZ, transcriptional coactivator with PDZ-binding motif; YAP, Yes-associated protein.

References

1. Dolecek, T. A., Propp, J. M., Stroup, N. E., and Kruchko, C. (2012) CBTRUS statistical report: Primary brain and central nervous system tumors diagnosed in the United States in 2005-2009. *Neuro Oncol.* **14 Suppl 5**, v1–v49
2. Tan, S. K., Jermakowicz, A., Mookhtiar, A. K., Nemeroff, C. B., Schürer, S. C., and Ayad, N. G. (2018) Drug repositioning in glioblastoma: A pathway perspective. *Front. Pharmacol.* **9**, 218

3. Dixon, S. J., Lemberg, K. M., Lamprecht, M. R., Skouta, R., Zaitsev, E. M., Gleason, C. E., Patel, D. N., Bauer, A. J., Cantley, A. M., Yang, W. S., Morrison, B., 3rd, and Stockwell, B. R. (2012) Ferroptosis: An iron-dependent form of nonapoptotic cell death. *Cell* **149**, 1060–1072
4. Lewerenz, J., Hewett, S. J., Huang, Y., Lambros, M., Gout, P. W., Kalivas, P. W., Massie, A., Smolders, I., Methner, A., Pergande, M., Smith, S. B., Ganapathy, V., and Maher, P. (2013) The cystine/glutamate antiporter system x(c)(-) in health and disease: From molecular mechanisms to novel therapeutic opportunities. *Antioxid. Redox Signal.* **18**, 522–555
5. Koppula, P., Zhuang, L., and Gan, B. (2021) Cystine transporter SLC7A11/xCT in cancer: Ferroptosis, nutrient dependency, and cancer therapy. *Protein Cell* **12**, 599–620
6. Dixon, S. J., and Stockwell, B. R. (2019) The hallmarks of ferroptosis. *Annu. Rev. Cell Biol.* **3**, 35–54
7. Meister, A., and Anderson, M. E. (1983) Glutathione. *Annu. Rev. Biochem.* **52**, 711–760
8. Hanes, C. S., and Hird, F. J. (1950) Synthesis of peptides in enzymic reactions involving glutathione. *Nature* **166**, 288–292
9. Griffith, O. W., Bridges, R. J., and Meister, A. (1978) Evidence that the gamma-glutamyl cycle functions *in vivo* using intracellular glutathione: Effects of amino acids and selective inhibition of enzymes. *Proc. Natl. Acad. Sci. U. S. A.* **75**, 5405–5408
10. Heisterkamp, N., Groffen, J., Warburton, D., and Sneddon, T. P. (2008) The human gamma-glutamyltransferase gene family. *Hum. Genet.* **123**, 321–332
11. Batsios, G., Najac, C., Cao, P., Viswanath, P., Subramani, E., Saito, Y., Gillespie, A. M., Yoshihara, H. A. I., Larson, P., Sando, S., and Ronen, S. M. (2020) *In vivo* detection of γ-glutamyl-transferase up-regulation in glioma using hyperpolarized γ-glutamyl-[1-^{13}C]glycine. *Sci. Rep.* **10**, 6244
12. Suzuki, H., and Kumagai, H. (2002) Autocatalytic processing of gamma-glutamyltranspeptidase. *J. Biol. Chem.* **277**, 43536–43543
13. West, M. B., Wickham, S., Quinalty, L. M., Pavlovicz, R. E., Li, C., and Hanigan, M. H. (2011) Autocatalytic cleavage of human gamma-glutamyl transpeptidase is highly dependent on N-glycosylation at asparagine 95. *J. Biol. Chem.* **286**, 28876–28888
14. Bansal, A., Sanchez, D. J., Nimgaonkar, V., Sanchez, D., Riscal, R., Skuli, N., and Simon, M. C. (2019) Gamma-glutamyltransferase 1 promotes clear cell renal cell carcinoma initiation and progression. *Mol. Cancer Res.* **17**, 1881–1892
15. Hayashima, K., Kimura, I., and Katoh, H. (2021) Role of ferritinophagy in cystine deprivation-induced cell death in glioblastoma cells. *Biochem. Biophys. Res. Commun.* **539**, 56–63
16. Bansal, A., and Simon, M. C. (2018) Glutathione metabolism in cancer progression and treatment resistance. *J. Cell Biol.* **217**, 2291–2298
17. Corti, A., Franzini, M., Paolicchi, A., and Pompella, A. (2010) Gamma-glutamyltransferase of cancer cells at the crossroads of tumor progression, drug resistance and drug targeting. *Anticancer Res.* **30**, 1169–1181
18. Briggs, K. J., Koivunen, P., Cao, S., Backus, K. M., Olenchock, B. A., Patel, H., Zhang, Q., Signoretti, S., Gerfen, G. J., Richardson, A. L., Witkiewicz, A. K., Cravatt, B. F., Clardy, J., and Kaelin, W. G., Jr. (2016) Paracrine induction of HIF by glutamate in breast cancer: EgIN1 senses cysteine. *Cell* **166**, 126–139
19. Goji, T., Takahara, K., Negishi, M., and Katoh, H. (2017) Cystine uptake through the cystine/glutamate antiporter xCT triggers glioblastoma cell death under glucose deprivation. *J. Biol. Chem.* **292**, 19721–19732
20. Yang, M., and Vousden, K. H. (2016) Serine and one-carbon metabolism in cancer. *Nat. Rev. Cancer* **16**, 650–662
21. Liu, X., Zhang, Y., Zhuang, L., Olszewski, K., and Gan, B. (2021) NADPH debt drives redox bankruptcy: SLC7A11/xCT-mediated cystine uptake as a double-edged sword in cellular redox regulation. *Genes Dis.* **8**, 731–745
22. Ji, Y., Wu, Z., Dai, Z., Sun, K., Zhang, Q., and Wu, G. (2016) Excessive L-cysteine induces vacuole-like cell death by activating endoplasmic reticulum stress and mitogen- activated protein kinase signaling in intestinal porcine epithelial cells. *Amino Acids* **48**, 149–156
23. Hughes, C. E., Coody, T. K., Jeong, M. Y., Berg, J. A., Winge, D. R., and Hughes, A. L. (2020) Cysteine toxicity drives age- related mitochondrial decline by altering iron homeostasis. *Cell* **180**, 296–310
24. Poltorack, C. D., and Dixon, S. J. (2021) Understanding the role of cysteine in ferroptosis: Progress & paradoxes. *FEBS J.* **289**, 374–385
25. Lieberman, M. W., Wiseman, A. L., Shi, Z. Z., Carter, B. Z., Barrios, R., Ou, C. N., Chévez-Barrios, P., Wang, Y., Habib, G. M., Goodman, J. C., Huang, S. L., Lebovitz, R. M., and Matzuk, M. M. (1996) Growth retardation and cysteine deficiency in gamma-glutamyl transpeptidase-deficient mice. *Proc. Natl. Acad. Sci. U. S. A.* **93**, 7923–7926
26. Rajpert-De Meyts, E., Shi, M., Chang, M., Robison, T. W., Groffen, J., Heisterkamp, N., and Forman, H. J. (1992) Transfection with gamma-glutamyl transpeptidase enhances recovery from glutathione depletion using extracellular glutathione. *Toxicol. Appl. Pharmacol.* **114**, 56–62
27. Hanigan, M. H. (1995) Expression of gamma-glutamyl transpeptidase provides tumor cells with a selective growth advantage at physiologic concentrations of cyst(e)ine. *Carcinogenesis* **16**, 181–185
28. Kawakami, K., Fujita, Y., Matsuda, Y., Arai, T., Horie, K., Kameyama, K., Kato, T., Masunaga, K., Kasuya, Y., Tanaka, M., Mizutani, K., Deguchi, T., and Ito, M. (2017) Gamma-glutamyltransferase activity in exosomes as a potential marker for prostate cancer. *BMC Cancer* **17**, 316
29. Horie, K., Kawakami, K., Fujita, Y., Matsuda, Y., Arai, T., Suzui, N., Miyazaki, T., Koie, T., Mizutani, K., and Ito, M. (2020) Serum exosomal gamma-glutamyltransferase activity increased in patients with renal cell carcinoma with advanced clinicopathological features. *Oncology* **98**, 734–742
30. Zhao, B., Wei, X., Li, W., Udan, R. S., Yang, Q., Kim, J., Xie, J., Ikenoue, T., Yu, J., Li, L., Zheng, P., Ye, K., Chinnaiyan, A., Halder, G., Lai, Z. C., *et al.* (2007) Inactivation of YAP oncoprotein by the Hippo pathway is involved in cell contact inhibition and tissue growth control. *Genes Dev.* **21**, 2747–2761
31. Reuven, N., Adler, J., Meltser, V., and Shaul, Y. (2013) The Hippo pathway kinase Lats2 prevents DNA damage-induced apoptosis through inhibition of the tyrosine kinase c-Abl. *Cell Death Differ.* **20**, 1330–1340
32. Pavel, M., Renna, M., Park, S. J., Menzies, F. M., Ricketts, T., Füllgrabe, J., Ashkenazi, A., Frake, R. A., Lombarte, A. C., Bento, C. F., Franze, K., and Rubinsztein, D. C. (2018) Contact inhibition controls cell survival and proliferation *via* YAP/TAZ-autophagy axis. *Nat. Commun.* **9**, 2961
33. Kobayashi, H., Takemura, Y., and Ohnuma, T. (1992) Relationship between tumor cell density and drug concentration and the cytotoxic effects of doxorubicin or vincristine: Mechanism of inoculum effects. *Cancer Chemother. Pharmacol.* **31**, 6–10
34. Westhoff, M. A., Zhou, S., Bachem, M. G., Debatin, K. M., and Fulda, S. (2008) Identification of a novel switch in the dominant forms of cell adhesion-mediated drug resistance in glioblastoma cells. *Oncogene* **27**, 5169–5181
35. Gujral, T. S., and Kirschner, M. W. (2017) Hippo pathway mediates resistance to cytotoxic drugs. *Proc. Natl. Acad. Sci. U. S. A.* **114**, E3729–E3738
36. Yamaguchi, I., Yoshimura, S. H., and Katoh, H. (2020) High cell density increases glioblastoma cell viability under glucose deprivation *via* degradation of the cystine/glutamate transporter xCT (SLC7A11). *J. Biol. Chem.* **295**, 6936–6945
37. Wu, J., Minikes, A. M., Gao, M., Bian, H., Li, Y., Stockwell, B. R., Chen, Z. N., and Jiang, X. (2019) Intercellular interaction dictates cancer cell ferroptosis *via* NF2-YAP signalling. *Nature* **572**, 402–406
38. Yang, W. H., Ding, C. K. C., Sun, T., Rupprecht, G., Lin, C. C., Hsu, D., and Chi, J. T. (2019) The Hippo pathway effector TAZ regulates ferroptosis in renal cell carcinoma. *Cell Rep.* **28**, 2501–2508
39. Yang, W. H., Huang, Z., Wu, J., Ding, C. K. C., Murphy, S. K., and Chi, J. T. (2019) A TAZ-ANGPTL4-NOX2 axis regulates ferroptotic cell death and chemoresistance in epithelial ovarian cancer. *Mol. Cancer Res.* **18**, 79–90
40. Katoh, Y., Michisaka, S., Nozaki, S., Funabashi, T., Hirano, T., Takei, R., and Nakayama, K. (2017) Practical method for targeted disruption of cilia-related genes by using CRISPR/Cas9-mediated homology-independent knock-in system. *Mol. Biol. Cell* **28**, 898–906
41. Shimomura, T., Hirakawa, N., Ohuchi, Y., Ishiyama, M., Shiga, M., and Ueno, Y. (2021) Simple fluorescence assay for cystine uptake *via* xCT in cells using selenocysteine and a fluorescent probe. *ACS Sens.* **6**, 2125–2128